VI International Conference on Computational Methods in Marine Engineering
MARINE 2015
F. Salvatore, R. Broglia and R. Muscari (Eds)

ACTIVE AND PASSIVE PITCH-CONTROLLED FLAPPING WING PROPULSORS; USAGE OF THE WAKE STRUCTURE AS A PERFORMANCE QUALIFIER

VASILEIOS T. TSARSITALIDIS[*], GERASIMOS K. POLITIS[†] AND KOSTAS A. BELIBASSAKIS[‡]

National Technical University of Athens
School of Naval Architecture & Marine Engineering
Heroon Polytechniou 9, Zografos 1580, Athens, Greece
email: [*]billtsars@gmail.com,[†] polit@central.ntua.gr, [‡]kbel@fluid.mech.ntua.gr

Key words: Biomimetic Marine Propulsors, Active/Passive Systems, Unsteady BEM

Abstract. Economic and ecological needs dictate for an ever growing need for increased efficiency, both in marine propulsion and energy saving systems. Biomimetic (flapping wing) systems, have already shown a serious potential as propulsors [1] and an even greater as a mechanism that converts energy from ship motions to thrust [2], [3]. In this paper, the problem of passively (spring loaded) or actively pitched controlled wing is formulated and solved using a free wake 3D Boundary Element Method [4]. For the spring loaded case, the unsteady BEM code is used to calculate the instantaneous forcing (i.e. pitching moment) entered in the nonlinear second order PDE in time, expressing equilibrium of moments including damping and inertia, around the pitch axis. Systematic simulations were conducted for a series of harmonically heaving wings of different aspect ratios, with the instantaneous pitch selected either passively via a spring-damper system or actively using a proper control algorithm. The results regarding developed mean thrust coefficient are presented in the form of systematic diagrams compatible with the design diagrams introduced in [1], allowing comparison of the different flapping wing propulsors. Results are also presented for the wake patterns of the different configurations, at similar propulsive conditions, revealing the connection between the propulsive effectiveness and 3D wake structure.

1 INTRODUCTION

Demand for low costs and regulations on emissions make an ever growing need for lower fuel consumptions of seagoing ships. On the other hand, increased safety requirements and passenger comfort at rough seas, necessitates improvements of their seakeeping characteristics. Under the light of the latest developments in both numerical investigations [1, 2, 3, 4, 5] and experiments [6]. Biomimetic Propulsion systems prove to have the potential of reducing the fuel requirements providing additional thrust in waves at the expense of ship

motions, reducing them in rough seas, providing thus the best compromise regarding fuel economy and seakeeping.

The modern history of biomimetics starts in 1935 with Gray's paradox, and theoretical developments start with the works of Sir James Lighthill [7] and T.Y. Wu [8]. A thorough review of those theories can be found in Sparenberg [9]. Extensive reviews of computational and experimental work in biomimetics can be found in the papers of Shyy et al [10] regarding aerodynamics and aeroelasticity; of M. Triantafyllou et al [11,12] regarding experimental developments and of Rozhdestvensky & Ryzhov [13] regarding all types of applications, even full scale, with additional care given to the work done by eastern scientists (i.e. Russians and Japanese).

The ability of the oscillating wing to absorb energy from wave induced ship motions and transform it to propulsive power gave rise to the idea for combined use of this system both as an energy saving device and as a control system for ship motions. As also reported in the extended review by Rozhdestvensky & Ryzhov [13], the Norwegian Fishing Industry Institute of Technology carried out full-scale tests of a passive propulsor, comprising two wings with elastic links, installed at the bow of a 180ton research fishing ship. The tests showed that the efficiency of such a propulsor reached up to 95% and it was demonstrated that it could be combined with a conventional screw propeller. At a speed of 15kn, in waves up to 3m height, a significant part (25%) of the thrust was provided by the wing propulsors. Using only the wing propulsor, at the same sea state, the ship was able to travel at speed up to 8kn. Furthermore, full-scale tests of a 174ton Russian research fishing vessel equipped with a wing device for extracting sea wave energy (see, e.g., [14]), showed that such a device could increase the delivered power up to 50-80% and reduce the ship motions by at least a factor of 2. Also, Japanese researchers used a suspended engine to oscillate a flapping wing system, [15]. Two different arrangements of the wing elements of the flapping propulsor have been considered. The first consists of two vertically mounted wings, operating in opposite phase, and the second of a horizontal wing, operating below a stationary plate. This engine-propulsor system was tested and the measured data show that it provides the same efficiency as a screw propeller, for an extended range of operating conditions. The above full-scale experiments confirm that the flapping wing, in some modes of operation, could be found to be equally effective as the typical marine propeller. However, by operating at lower frequency it has the advantage to excite less noise and vibration. Apparently, there is already strong evidence about the good performance and capabilities of the proposed system, dictating the need for the development of tools for the hydrodynamic analysis and design of such systems.

The scope of the present work is: (a) to show some numerical simulations of the performance of biomimetic (flapping wing) systems under either Passive Pitch Control (PPC) (i.e. spring-damper loaded) or Active Pitch Control (APC) and (b) to propose the use of the 3D structure of the free wake of such systems as a qualifier regarding its optimum performance. To this end the unsteady boundary element code with free wake UBEM [4] has been coupled with a 1-DOF hydro-elastic model of a spring driven wing, to dynamically calculate its pitch in time. In addition a new APC algorithm has been proposed on the basis of the heaving history of the wing, following the lines of thought in Politis and Politis [2]. Presented results indicate that both PPC and APC biomimetic wings can have substantial abilities as ship propulsors with the APC to be the best. Furthermore APC wing wakes are ruled from well-formed alternating

ring shaped free vortex trains (3D analog of the 'inverse Karman Vortex Street'), with much smaller transition regions than that observed in PPC wings.

2 FORMULATION

2.1 Wing geometry, motion and panel generation

For the general case of a flapping wing configuration, the independent variables which define the state of the system can be decomposed in two groups. The 'geometric' variables and the 'motion related' variables. For the selection of wing geometry the flapping wing series described in Politis and Tsarsitalidis [1] has been used. More specifically we have chosen wings with: $s/c = 2,4,6$ where s denotes span and c the chord length. The outline and meshing of the wing is presented in Figure 1 for the case $s/c = 4$. A NACA0012 profile throughout the span is used for all cases. Finally to the geometric variables we have to add the pitching axis position and elastic data. This is the subject of the later section 2.4.

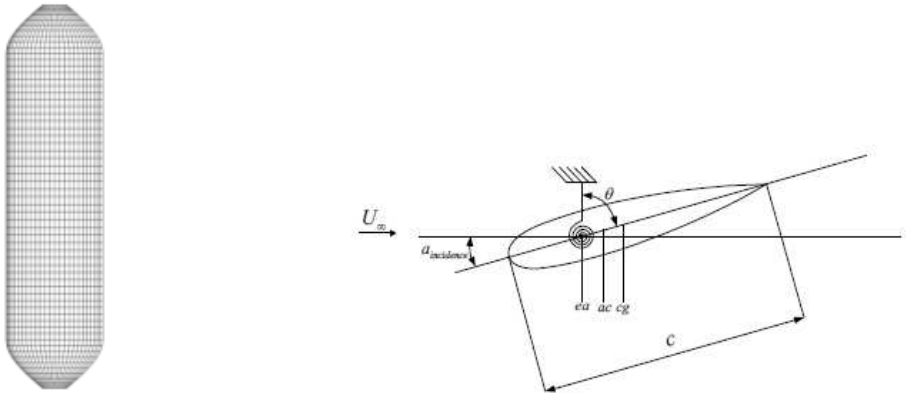

Figure 1: Planform of a straight wing s/c=4.0 (left), and 1 DoF hydroelastic model (right).

Regarding description of wing motion, for the cases considered in this paper, they can be decomposed in a translational part with velocity of advance U, a heaving part with instantaneous heaving amplitude $h(t)$ and a pitching motion with instantaneous pitch angle $\theta(t)$. For the simplest 'prescribed motion' case, heaving and pitching can be independent harmonic (sinusoidal) functions of frequency f with amplitudes h_0, θ_0 and some phase angle ψ between them (in the current paper $\psi = 90^0$). For the most advanced cases considered in this work, i.e. the spring loaded and the actively pitched wing, the pitching motion is dependent from the heaving motion in general in a complex way. More specifically for the spring loaded case instantaneous pitch is a result of the instantaneous equilibrium of moments, equation (4). In this case the properties of the spring/damper system (elastic constant K and damping factor C) act as parameters for the calculated instantaneous pitch. For the actively pitched wing, instantaneous pitch is selected as a function of the time rate of heave and the velocity of advance Politis&Politis [2].

With the motion parameters known, the instantaneous angle of attack $a(t)$ of each wing with respect to the undisturbed flow is given by:

$$a(t) = \theta(t) - \tan^{-1}\left(\frac{dh(t)/dt}{U}\right) \tag{1}$$

Additionally, as in previous works, *Str* denotes the Strouhal number defined by:

$$St = \frac{f \cdot h}{U}, h = 2h_0 \tag{2}$$

and h denotes the heave height. Finally, the Thrust coefficient is defined as

$$C_T = \frac{T}{0.5\rho U^2 S} \tag{3}$$

where T the calculated mean thrust and S the swept area covered by the wing in motion, given by $S = s \cdot 2h$.

2.2 Spring loaded wing simulations

In order to find the pitching angle at each moment, the following differential equation has to be solved for $\theta(t)$

$$M_{ext}(t) = I\ddot{\theta}(\mathrm{t}) + C\dot{\theta}(\mathrm{t}) + K\theta(\mathrm{t}) \tag{4}$$

where M_{ext} is the external moment (in the specific case, the hydrodynamic moment), *I* the moment of inertia about z axis, *C* the damping factor and *K* the spring stiffness.

The solution of the coupled problem is obtained by an explicit scheme, where the hydrodynamic moment $M_{ext}(t)$ calculated at each step is used in order to find the pitch angle for the next time step. As long as the time step is small enough and pitch angle variations are also small, this scheme is expected to be robust and accurate. For the time integration of (4) a Newmark -β scheme is applied. [16].

Regarding wing geometry and properties we have worked as follows: For the wing, an initial geometry is selected to be that of a straight foil with $s/c = 2, 4, 6$ and a mass distribution resembling that of an aluminum shell of the same shape was assumed. Then, the mass, center of mass and moment of inertia can be calculated by employing a CAD software and numerical integrations or empirical rules (found in textbooks) for simple geometries. As concerns the selection of the damping factor we worked as follows: As it is known from the dynamics of harmonic oscillators,

$$\zeta = \frac{C}{2\sqrt{IK}} \tag{5}$$

is called the 'damping ratio'. The value of the damping ratio ζ critically determines the behavior of the system. A damped harmonic oscillator can be *Overdamped* (ζ>1, *Critically damped* (ζ =1) or *Underdamped* (ζ<1). It is desirable that the system is not allowed to

resonate with the excitation, but also that it does not delay to respond. Thus, $\zeta=1$ was chosen as a parameter for the initial explorations. From a known ζ, the corresponding damping factor C can be calculated for each setting of K, which will be chosen to vary for the systematic simulations.

2.3 Active Pitch Control

It is known from the literature that spring loaded wings operate well in a narrow area of conditions. Thus it was deemed necessary to develop an active pitch control algorithm, in order to cover for a wider range. For the specific application, the simple open loop algorithm presented by Politis and Politis [2] is employed and evolved as follows:
From the original of Politis and Politis [2], the pitch angle at each step is defined as:

$$\theta(t) = w\tan^{-1}\left((dh/dt)/U\right) \tag{6}$$

where w is a 'pitch control parameter' ranging from zero to one that is set beforehand. Knowing the expected heave amplitude, frequency and speed of advance, and knowing that:

$$a(t) = (1-w)\tan^{-1}\left((dh/dt)/U\right) \tag{7}$$

the parameter w can be set to a number that the maximum angle of attack does not exceed a definite value. Closer examination of (7), leads to the realization that $\tan^{-1}\left((dh/dt)/U\right)$ gives the angle of the undisturbed flow and that decrease in the value of w, increases the angle of attack. If the constant parameter w is substituted with a variable $w(t)$ and keeping in mind the objective of keeping the angle of attack below a given value, a new law for $w(t)$ can be obtained by finding the lowest $w(t)$ satisfying the inequality:

$$A \geq \left(1-w(t)\right)\tan^{-1}\left(dh/dt/U\right), A = given \tag{8}$$

The value found, is then substituted in (6), to give the pitching angle. This gives at a minimal addition of computational cost, a different to that used in Politis&Politis [2], non-harmonic profile of pitching motion, where the angle of attack is kept below the given value, but also equal to it for a longer time. It should be noted, that when the angle of the undisturbed flow is smaller than the desired angle of attack (and when it changes from the positive to negative –one side of foil to the other-) it is better to keep the foil at a zero pitch angle, something that this algorithm follows very well.

2.4 Selection of Pitching Axis Position and unsteady center of pressure

For the selection of the pitching axis position the requirement of stable motion patterns, leads to select it in front of the center of pressures. From linear, steady 2D wing theory it is known that the center of pressures coincides with the one quarter chord from the leading edge. In our case the wing performs large nonlinear motions and thus a preliminary investigation is required to confirm (or not) the results from linear theory. By analyzing the results from

existing prescribed motion simulations Politis & Tsarsitalidis [1] and applying $d(\mathrm{t}) = M_z(\mathrm{t}) / F_y(t)$ ($M_z(\mathrm{t})$ is the hydrodynamic moment around the selected pitch axis of the wing, $F_y(t)$ is the hydrodynamic force) the time dependent position of the aerodynamic center from the selected pitch axis of the wing $d(\mathrm{t})$ can be found. In Figure 2, results of these calculations are shown for a multitude of different prescribed motion simulations, as taken from previous works (one line-type for each simulation) for the pitching axis positioned at 0.3c from the leading edge. The peaks of the lines should be disregarded, as they are the result of very small F_y at the upper and lower points of the oscillation. From the main part of the curves, it can be concluded that the hydrodynamic center resides slightly ahead of 0.3c for most of the time for all cases. Similar calculations (not included here) for the pitching axis positioned at 0.2c from the leading edge, confirm this result and additionally indicate that the position of the pitching axis has a secondary effect on the position of the center of pressures. After this analysis, we have chosen the pitching axis at 0.25c from leading edge, for both minimization of moments as well as stability considerations. It should be noted that a position much closer to the le, could mean large moments, which could lead to strong responses and instabilities, difficult to solve.

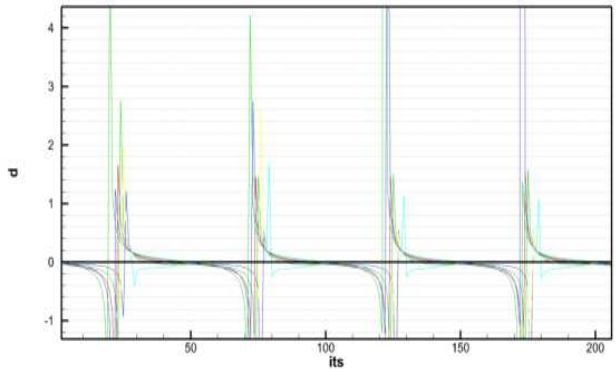

Figure 2: Histories of position of the hydrodynamic center, relative to the pitching axis, for pitch axis at 0.3c from leading edge (Negative is for forward).

3 RESULTS AND DISCUSSION

3.1 Spring Loaded Wing Systematic Simulations

Systematic simulations for $Str = 0.2 \div 0.7$ and varying K/ρ (ρ denotes the fluid density in kg/m^3, i.e. $\rho = 1000\, kg/m^3$), are used to produce Figure 3 ($s/\mathrm{c} = 2, K/\rho = 1 \div 20$), Figure 4 ($s/\mathrm{c} = 4, K/\rho = 1 \div 20$) and Figure 5 ($s/\mathrm{c} = 6, K/\rho = 5 \div 90$). In all cases a sinusoidal heaving motion is used with $h/c = 2$. Those figures are similar to the systematic charts in Politis&Tsarsitalidis [1], with the difference of having in the horizontal axis K/ρ (instead of θ). Notice that K/ρ is the pitch defining parameter for this problem, since all other parameters are either constants or functions of K. From figures 3, 4 and 5 we conclude that substantial thrust can be produced for all the three cases. Comparing hydrodynamic

efficiencies we observe that the wing with the greatest aspect ratio $s/c = 6$, succeeds the better efficiency (about 68%, figure 5). Finally the effect of the spring stiffness K seems to play a secondary role at constant Strouhal, for all cases. This result is connected with a selection of critical damping in all cases. The effect of parameters such as pitching axis position, damper settings with possibly non-linear springs and dampers and different wing shapes have to be investigated, but the existing empirical knowledge, that spring loaded wings operate well in limited conditions, is confirmed.

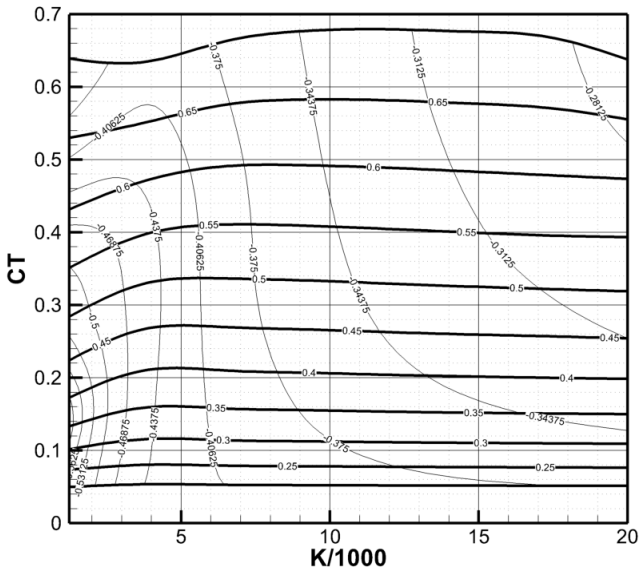

Figure 3: $Ct - K$ chart for a straight wing s/c=2, h/c=2.0, under simple harmonic heaving motion. Thick lines are used to indicate for Strouhal number and thin lines efficiency, respectively.

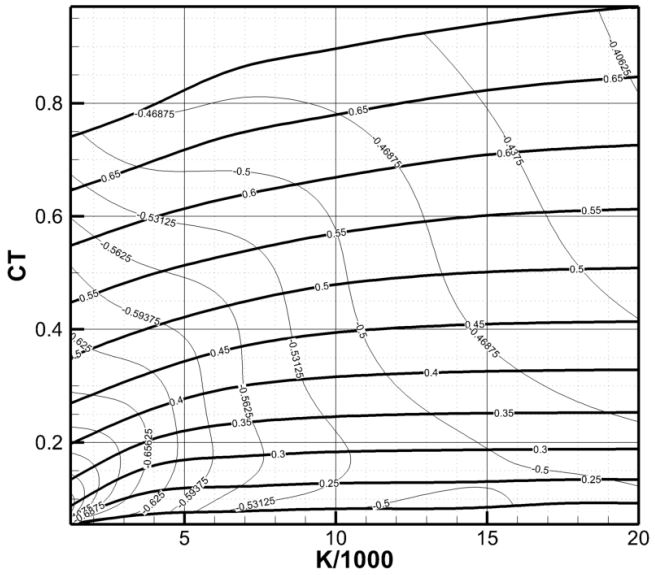

Figure 4: $Ct - K$ chart for a straight wing s/c=4, h/c=2.0, under simple harmonic heaving motion. Thick lines are used to indicate for Strouhal number and thin lines efficiency, respectively.

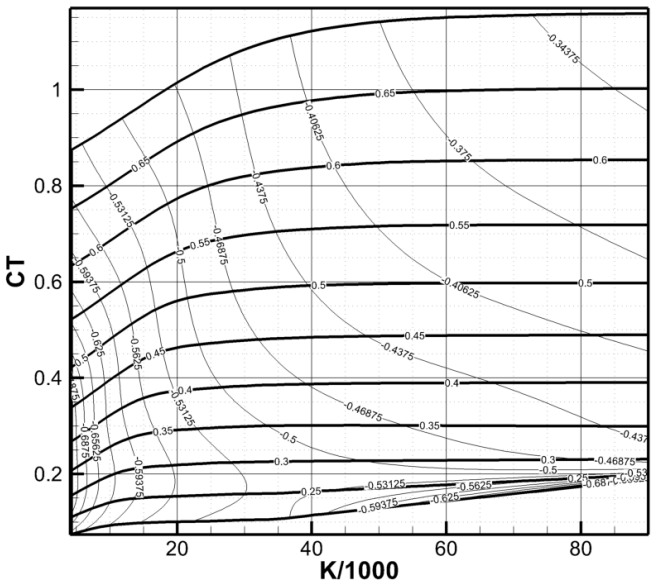

Figure 5: $Ct-K$ chart for a straight wing s/c=6, h/c=2.0, under simple harmonic heaving motion. Thick lines are used to indicate for Strouhal number and thin lines efficiency, respectively.

3.2 Active Pitch Control Systematic Simulations

Systematic simulations for varying Str and target $A_{\max} = 4^0 \div 20^0$ for an actively pitched wing are presented in Figure 6 ($s/c = 2$, $Str = 0.2 \div 0.6$), Figure 7 ($s/c = 4$, $Str = 0.2 \div 0.7$) and Figure 8 ($s/c = 6$, $Str = 0.2 \div 0.6$). In all cases a sinusoidal heaving motion is used with $h/c = 2$, while the APC relation (8) has been used for the instantaneous pitch setting. Those figures are similar to the systematic charts in Politis&Tsarsitalidis [1], with the difference of having in the horizontal axis $A_{\max}$ instead of the pitch angle amplitude θ. The vertical axis of the figures shows the succeeded thrust coefficient Ct while thicker lines are for constant Strouhal and thinner lines are for constant efficiency. From each figure (i.e. given $s/c, h/c$) we observe that increasing the $A_{\max}$, thrust coefficient is increased as expected. Furthermore, by increasing aspect ratio (i.e. s/c) the developed thrust coefficient is increased for the same Str and $A_{\max}$ as expected. Finally much larger hydrodynamic efficiencies are succeeded in all actively pitched cases (figures 6, 7 and 8) compared to the passively pitched case (figures 3, 4 and 5). More specifically efficiencies as large as 80% are observed (figure 8) while the $A_{\max}$ range with good efficiencies is satisfactorily wide.

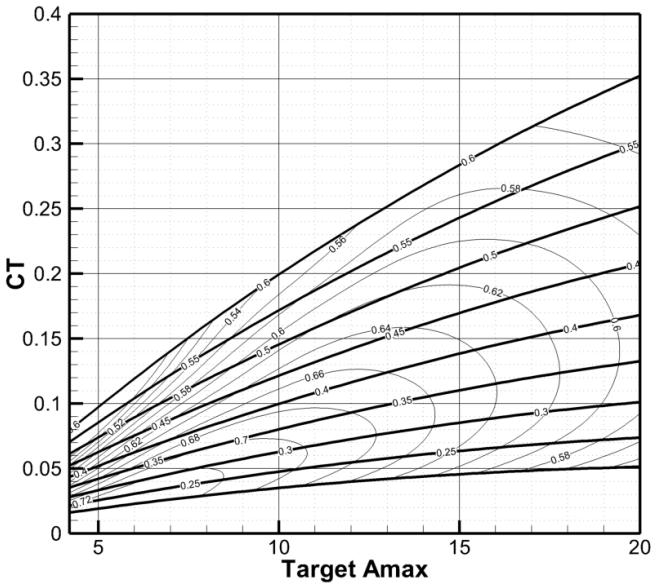

Figure 6: Ct-Target A_{max} chart for a straight foil s/c=2, h_0/c=2, under simple harmonic motion. Thick lines are used to indicate for Strouhal number and thin lines efficiency, respectively.

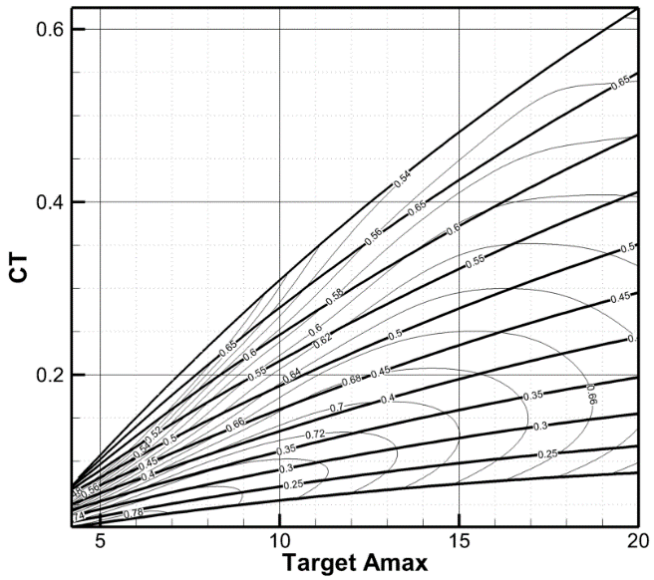

Figure 7: Ct-Target A_{max} chart for a straight foil s/c=4, h_0/c=2, under simple harmonic motion. Thick lines are used to indicate for Strouhal number and thin lines efficiency, respectively.

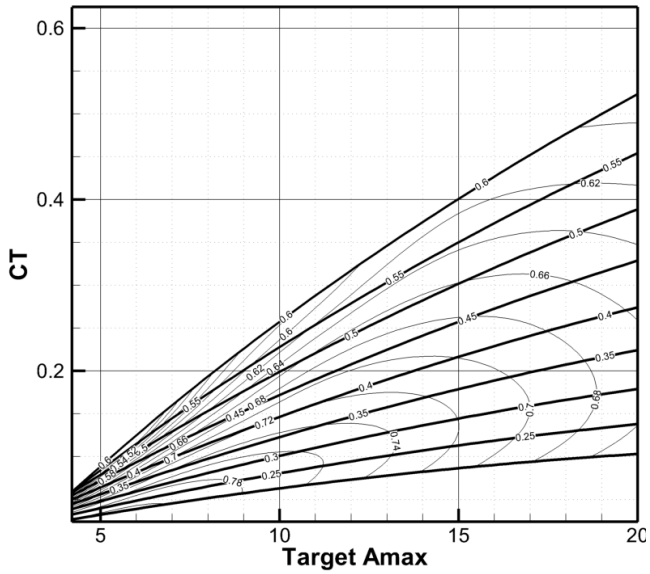

Figure 8: Ct-Target A_{max} chart for a straight foil s/c=6, h_0/c=2, under simple harmonic motion. Thick lines are used to indicate for Strouhal number and thin lines efficiency, respectively.

3.3 Using the wake structure as a hydrodynamic performance qualifier

In the plots in Figs. 9 and 10 we present the unsteady wake roll-up for four cases. More specifically, Fig. 9 shows the wake structure of a passively pitched wing while Fig. 10 the corresponding wake structure of an actively pitched wing. The shown surfaces are the trace in time of the vorticity created at the trailing edge of the thrust producing biomimetic wings, as calculated by applying the vorticity transport equation at each time step. The surfaces are colored by the dipole intensity μ. Since the surface vorticity $\vec{\gamma}$ is connected with the surface gradient of μ through $\vec{\gamma} = \vec{n} \times \nabla \mu$ ($\vec{n}$ denotes a unit normal vector to the μ surface), constant μ lines on this surface visualize the (surface) vortex lines (i.e. $\vec{\gamma}$ is tangential to the constant μ lines). With the aid of Figures 9 and 10, we visualize the train of alternating ring-shaped vortices ('inverse Karman vortex street') in the wake of each of our biomimetic wings. Since the produced thrust of each wing is connected with the energy contained in the jet produced by each ring vortex and since the ring vortices of the Active Pitch Controlled wing are more well-formed and larger in extend than the corresponding vortices of the Passive Pitch Controlled wing, we conclude (using momentum considerations) that the APC should have better hydrodynamic performance than the PPC wing. Since this result is confirmed by quantitative calculations (figure 3 to 8), we conclude that the wake structure can be used as a qualifier of the biomimetic wing hydrodynamic performance.

4. CONCLUSIONS

An initial study of the potential of wings with passive (spring loaded) and active pitch control has been presented with application to marine propulsion. Both systems seem promising, with

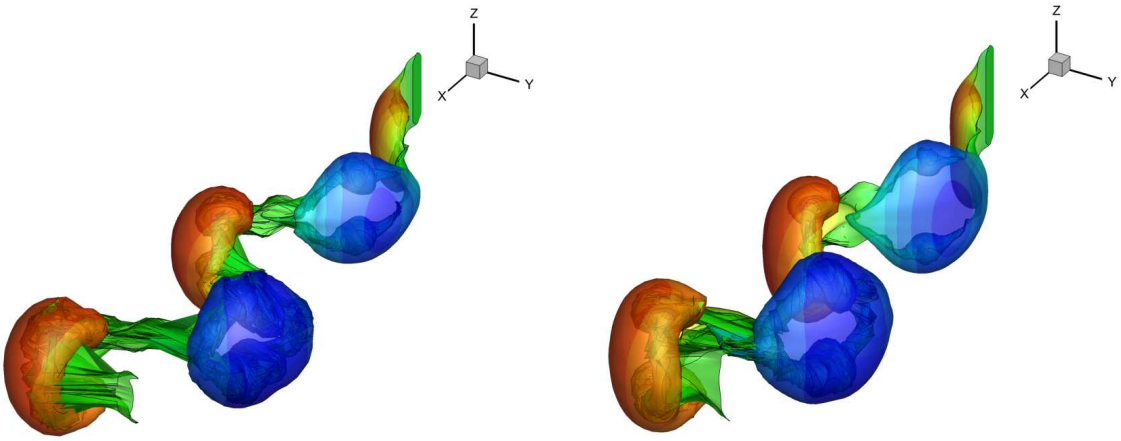

Figure 9: Spring loaded wing, with parameters $s/c = 4, h/c = 2, Str = 0.3, K/\rho = 4$ (left), and $s/c = 6, h/c = 2, Str = 0.3, K/\rho = 6$ (right)

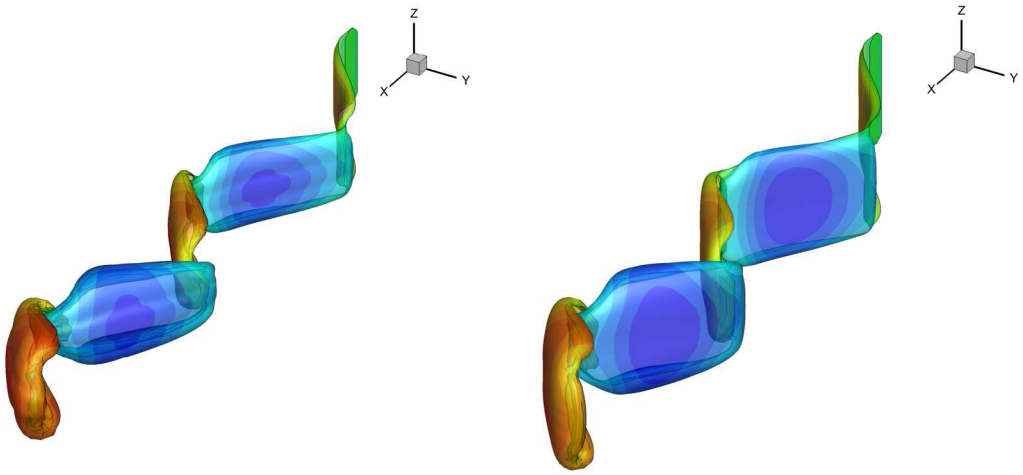

Figure 10: APC wing, with parameters $s/c = 4, h/c = 2, Str = 0.3, A_{\max} = 7^0$ (left) and $s/c = 6, h/c = 2, Str = 0.3, A_{\max} = 7^0$ (right).

the actively controlled being more adaptable, but with the spring loaded independent of electronics and mostly predictable. Systematic simulations were conducted for a series of harmonically oscillating wings of different aspect ratios, with the instantaneous pitch selected either passively via a spring-damper system or actively using a proper control algorithm. Results concerning mean thrust coefficient are presented in the form of systematic diagrams compatible with the design diagrams introduced in [1], allowing comparison of the different flapping wing propulsors. Results are also presented for the wake patterns of the different configurations, at similar propulsive conditions, revealing the connection between the propulsive effectiveness and 3D wake structure.

ACKNOWLEDGEMENT

This research has been co-financed by the European Union (European Social Fund – ESF) and Greek national funds through the Operational Program "Education and Lifelong Learning" of the National Strategic Reference Framework (NSRF) 2007-2013: Research Funding Program ARISTEIA - project BIO-PROPSHIP: «Augmenting ship propulsion in rough sea by biomimetic-wing system».

REFERENCES

[1] Politis, G.K., Tsarsitalidis V.T., Flapping wing propulsor design: An approach based on systematic 3D-BEM simulations. *Ocean Engineering* (2014) **84**: 98-123.
[2] Politis, G., Politis K., Biomimetic propulsion under random heaving conditions, using active pitch control. *Journal of Fluids and Structures* (2014). **47**: 139-149.
[3] Belibassakis, K.A., Politis G.K., Hydrodynamic performance of flapping wings for augmenting ship propulsion in waves. *Ocean Engineering* (2013) **72**: 227-240.
[4] Politis, G.K., Application of a BEM time stepping algorithm in understanding complex unsteady propulsion hydrodynamic phenomena. *Ocean Engin.* (2011). **38**(4): 699-711.
[5] Belibassakis, K.A., Politis G.K., Hydrodynamic analysis of flapping wing systems for augmenting ship propulsion in rough sea. Proc. 22 *Intern. Ocean and Polar Engineering Conference* (ISOPE 2012).
[6] Bøckmann, E., S. Steen, Experiments with actively pitch-controlled and spring-loaded oscillating foils. *Applied Ocean Research* (2014) **48**: 227-235.
[7] Lighthill, J., *Aquatic Animal Locomotion.* (1973) 1973.
[8] Wu, T.Y., Hydromechanics of swimming propulsion. Part 1. Swimming of a two-dimensional flexible plate at variable forward speeds in an inviscid fluid. *J. Fluid Mech,* (1971) **46**: 337–355.
[9] Sparenberg, J.A., Survey of the mathematical theory of fish locomotion. *Journal of Engineering Mathematics* (2002) **44**(4): 395-448.
[10] Shyy, W., et al., Recent progress in flapping wing aerodynamics and aeroelasticity. *Progress in Aerospace Sciences* (2010) **46**(7): 284-327.
[11] Triantafyllou, M.S., Triantafyllou G.S., Gopalkrishnan R., Wake mechanics for thrust generation in oscillating foils. *Physics of Fluids A* (1991) **3**(12): 2835-2837.
[12] Triantafyllou, M.S., Techet A.H., Hover F.S., *Review of experimental work in biomimetic foils. IEEE Journal of Oceanic Engineering* (2004) **29**(3): 585-594.
[13] Rozhdestvensky, K.V., Ryzhov V.A., Aerohydrodynamics of flapping-wing propulsors. *Progress in Aerospace Sciences*, (2003) **39**(8): 585-633.
[14] Nikolaev, M.N., Savitskiy A.I., Senkin Y.U.F., Basics of calculation of the efficiency of a ship was propulsor of the wing type. *Sudostroenie* (1995) **4**: 7-10.
[15] Isshiki, H. Wave energy utilization into ship propulsion by fins attached to a ship. in *Proc. of the International Offshore and Polar Engineering Conference* (ISOPE1994).
[16] Chopra, A.K., *Structural Dynamics* (2007).